Sustainable Environmental Insight

Review
Volume 2(2), 2025, 83–97
https://doi.org/10.53623/sein.v2i2.789

Phorboxazole A: Comparative Synthetic Approaches, Bioactivity, and Future Green Chemistry Strategies

Jovale Vincent Tongco

Department of Forest, Rangeland and Fire Sciences, University of Idaho, Moscow, ID, 83844 USA

Correspondence: jtongco@uidaho.edu

SUBMITTED: 28 July 2025; REVISED: 28 August 2025; ACCEPTED: 30 August 2025

ABSTRACT: Phorboxazole A is a tropical marine macrolide isolated from the sponge *Phorbas* sp. and has emerged as one of the most potent cytostatic agents found in nature, with nanomolar activity against diverse cancer cell lines and antifungal properties against pathogens like *Candida albicans*. The structural complexity of Phorboxazole A, characterized by a 46-carbon skeleton, 28 stereocenters, two oxazole rings, and a macrocyclic core, has spurred innovative synthetic campaigns since its isolation 30 years ago. This review article highlights the approaches in total synthesis strategies for phorboxazole A, emphasizing the Petasis-Ferrier union/rearrangement, tri-component coupling, convergent assembly, stereoselective cyclization, and comparative retrosynthetic analysis, followed by discussions regarding its biological activity, and the feasibility of utilizing green chemistry principles in mitigating the hazardous effects on human health and the environment.

KEYWORDS: Total synthesis; phorboxazole; macrolides; green chemistry; *Phorbas* sp.

1. Introduction

Marine sponges are rich sources of important natural products with applications in medicine and health. (+)-Phorboxazole is a naturally occurring isomeric oxazole-containing macrolide (class of antibiotics used to manage and treat various infections [1–4]) initially isolated by Searle and Molinsky [5] from a particular marine sponge endemic to the western coast of Australia and Eastern Indian Ocean (*Phorbas* sp.). Oxazoles are heterocyclic aromatic compounds homologous to azoles, but with an O and N separated by a carbon atom [6–8]. It exists as an enantiomeric compound, exhibiting chirality on a distinct site. One carbon of Phorboxazole is a chiral center, meaning it exists in two forms, namely Phorboxazole A and Phorboxazole B. Figure 1 shows the chiral center C13 of Phorboxazole A. Of the two enantiomers of Phorboxazole, it was reported that Phorboxazole A demonstrated potency against human cancer cell cultures [9, 10]. It has been shown to deter cell cycle in the S phase without affecting tubulin polymerization. The S phase (synthesis phase) of the cell cycle is crucial because in this step, DNA is replicated [11, 12]. A cancer cell not undergoing efficient

S phase in their cell cycle leads to minimized duplication and ultimately to its imminent death [13–15]. Beyond cancer research, phorboxazole A inhibits *C. albicans* at 1.0 μg/mL, with retained efficacy against fluconazole-resistant strains [9, 16]. Phorboxazole A was also shown to selectively arrest Burkitt lymphoma CA46 cells in the S-phase, distinct from tubulin-targeting agents like taxanes [17]. This unique mechanism, coupled with picomolar GI50 values across the NCI-60 panel, makes it a suitable candidate for developing novel antimitotics [18, 19]. An issue with using Phorboxazole A for medicinal purposes is its scarcity. *Phorbas* sp. is a rare organism, often found in deep and unusual places in the ocean [20, 21]. With the degree of difficulty in undertaking natural isolation of Phorboxazole, it has come to the attention of several synthetic chemists to synthesize Phorboxazole A in the laboratory and examine its biological activity and chemical properties more thoroughly. Synthetic laboratories of Smith [22] and Williams [23] pioneered the successful synthesis of Phorboxazole A utilizing different approaches. This review focuses on: 1) the comparative analysis on the foundational and landmark approaches to Phorboxazole A by the groups of Smith and Williams, including the biomimetic approach employed by the Forsyth group; 2) the biological activity of Phorboxazole A, particularly against cell lines and fungi; and 3) the future perspectives in employing green chemistry strategies in the total synthesis of phorboxazole A, such as the use of green organocatalysts, reduced catalytic loads, and alternative solvents, to help minimize the harmful effects of the materials and processes involved on human health and the environment.

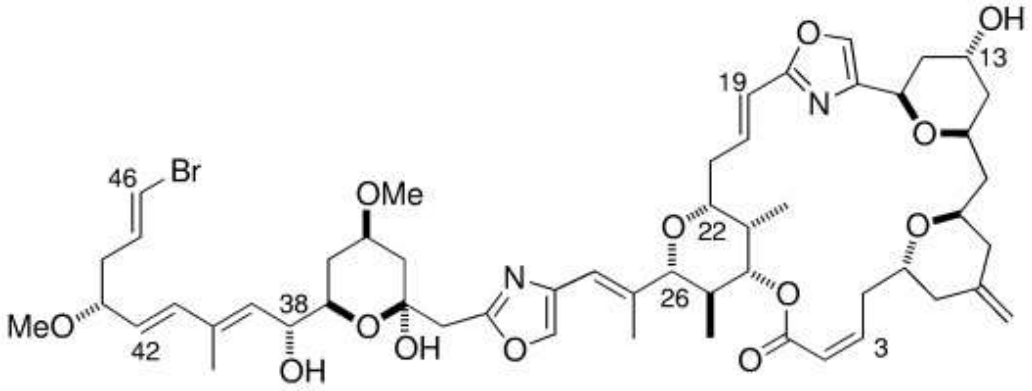

Figure 1. Phorboxazole A (*Reprinted with permission [23]*).

2. Petasis-Ferrier Union/Rearrangement

The Smith group started to embark on the synthesis of this remarkable compound shortly after Searle and Molinsky isolated it in 1995 [5]. They started working on the synthesis of this compound in 1997. The first total synthesis of Phorboxazole A was reported by the Forsyth group [24], then the total synthesis of Phorboxazole B followed shortly thereafter and was reported by Evans and Fitch [25]. The Forsyth group pioneered a tri-component coupling strategy that divides phorboxazole A into three fragments: C3–C17, C18–C30, and C31–C46. The key to this approach is the biomimetic formation of both oxazole rings via oxidation-cyclodehydration of serine-derived amides, mirroring non-ribosomal peptide synthase/polyketide synthase (NRPS/PKS) biosynthesis [26–28]. The Forsyth group method exhibits modularity, facilitating analog synthesis, such as C45–C46 vinyl chloride derivatives, which display picomolar cytotoxicity [19]. The Smith group used and exploited a modified

Petasis-Ferrier union/rearrangement tactic for a stereo-controlled construction of two *cis*-fused tetrahydropyrans at C11–C15 and C22–C26. Figure 2 shows the retrosynthetic analysis of the total synthesis of Phorboxazole A employed by the Smith group. The figure also shows the differences between Phorboxazoles A and B, particularly the stereochemistry of functional groups at C13.

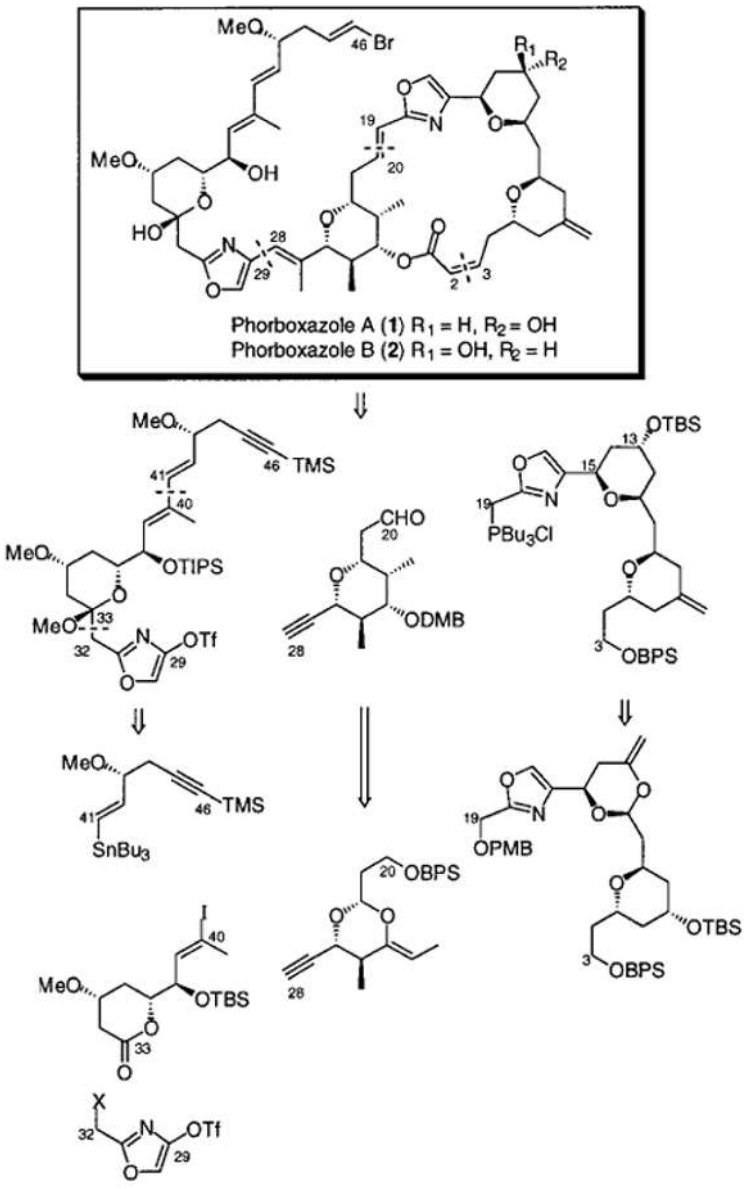

Figure 2. Retrosynthetic analysis of Phorboxazole A (and B) (Reprinted with permission [22]).

From the retrosynthetic perspective, disconnections of Phorboxazole A at the C1 macrolactone, the C23 and C28–C29 linkages led to side chain subtarget 3 and macrolide precursor 4. A Wittig transform at C19–C20 further dissected 4 into aldehyde 5 and salt 6, the syntheses of which were described previously. Continuing with this analysis, disconnection of subtarget 3 at C32–C33 and C40–C41 revealed vinyl stannane 7, vinyl iodide 8, and the bifunctional oxazole 9. Construction of the C40–C41 linkage would entail a Stille coupling, while oxazole 9, possessing the pseudobenzylic bromide and the triflate moieties, was envisaged as a novel bidirectional linchpin to unite the side chain with the macrocycle.

Importantly, the coupling strategy possessed considerable flexibility from a tactical perspective. Supplementary Material (SM) Figures 1–6 summarize the total synthesis of Phorboxazole A by the Smith group.

3. Convergent assembly

The Williams group designed the total synthesis of Phorboxazole A via the convergent assembly of four non-racemic components. These four racemic components are labeled 2–5 on the retrosynthetic analysis done by the Williams group, as shown in SM Figure 7. Stereoselective formation of the C22–C26 tetrahydropyran moiety of the target molecule was the central issue for their design strategy (components 3 and 4). They utilized the Horner-Wadsworth-Emmons reaction, forming the fully substituted pyran, retaining the stereochemistry of C22 of component 3 in the π-allyl cation cyclization [29]. C3–C19 bispyran component 5 was assembled using an enantio-controlled procedure via asymmetric allylation. Other important reactions in their synthesis include the use of Wittig reaction [30–33] for constructing the *E*-C19–C20 alkene, followed by the subsequent attachment of the labile C42–C46 segment by a modified Julia olefination. Their strategy culminated in late-stage macrocyclization by installation of the (*Z*)-C2–C3 enolate. The summary of the total synthesis of Phorboxazole A by the Williams group is shown in SM Figures 8 and 9. The C28–C41 aldehyde yield was 39% from the β,γ-unsaturated aldehyde (component 6), while the overall yield of Phorboxazole A after deprotection using 6% aqueous HCl in THF is 80%. Synthetic material was identical in all respects with spectroscopic, chemical, and physical data provided for the natural product.

4. Importance of the Petasis-Ferrier union/rearrangement

The Petasis-Ferrier rearrangement is an important part of both the synthetic pathways of Smith and Williams. It enables the assembly of the fused tetrahydropyran rings into a chain from C3–C19 of the target molecule, a part of the molecule that contains most of its functionality, including the chirality on C13. Controlled use (modification) of the Petasis-Ferrier rearrangement produced the *cis*-tetrahydropyran necessary for the synthesis of the target molecule. Figure 3 depicts the mechanism of the two types of Ferrier rearrangement. Type I was proposed by Petasis in 1995, and this is the one used by both the Smith and Williams groups for their total synthesis of Phorboxazole A. Type II was proposed earlier (1979) by Ferrier [34, 35]. This one was not used because it produces a cyclic ketone with a hydroxyl group on the third carbon. Collectively, these two Ferrier-type reactions are known as Petasis-Ferrier union/rearrangement reactions. The type I Petasis-Ferrier rearrangement is stereochemically beneficial because it preserves existing stereocenters in the starting material while forming the necessary tetrahydropyran ring structure, proceeding through an oxocarbenium ion intermediate. More importantly, the substituents on the ring that are not directly involved in the reaction maintain their original stereochemical configuration. This allowed the groups to use chiral starting materials and transfer that chirality into the final product, which was essential for establishing the specific chirality at C13 in Phorboxazole A. Meanwhile, The type II rearrangement is unsuitable because it completely changes the molecule's core structure. It breaks the pyran ring and rearranges it into a carbocyclic ketone.

This process destroys the desired tetrahydropyran ring and eliminates the stereocenter at the carbon that becomes part of the ketone's carbonyl group (C=O), failing to generate the required precursor for the synthesis.

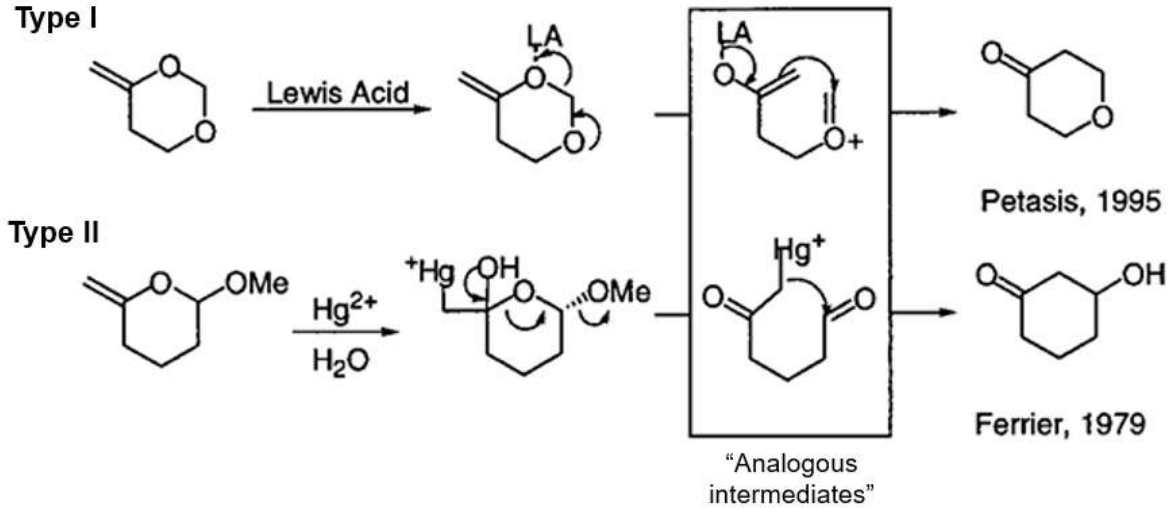

Figure 3. Mechanism of Ferrier type I and type II rearrangements, collectively known as Petasis-Ferrier union/rearrangement (Reprinted with permission [22]).

5. Comparative retrosynthetic analysis

Summarized in Figures 4 and 5 is the comparison of the bond breakage analysis used by Smith and Williams, respectively. Shown are the parts where Phorboxazole A bonds were broken (Blue line: Smith group, Red line: Williams group) during retrosynthetic analysis to identify possible synthons and synthetic equivalents. The chain from C29–C40 is broken down into two smaller components. The Smith group came up with five possible components to assemble the target molecule. The Horner-Wadsworth-Emmons (HWE) reaction is the chemical reaction of stabilized phosphonate carbanions with aldehydes (or ketones) to produce predominantly E-alkenes [29, 36]. Julia olefination is a chemical reaction of phenyl sulfones with a carbonyl group to form an alkene [37–40]. The general reaction for Julia olefination is shown in SM Figure 10, where it was applied to a sulfone component numbered C42–C46, so it can be attached to the component C28–C41. This forms the C41–C42 double bond in the target molecule. The corresponding components/sub-targets proposed by both groups are shown in Figure 6. The high E-selectivity and mild conditions of the HWE reaction and the reliability of the modified Julia olefination for coupling complex fragments were the reason why these steps were chosen over alternative coupling methods.

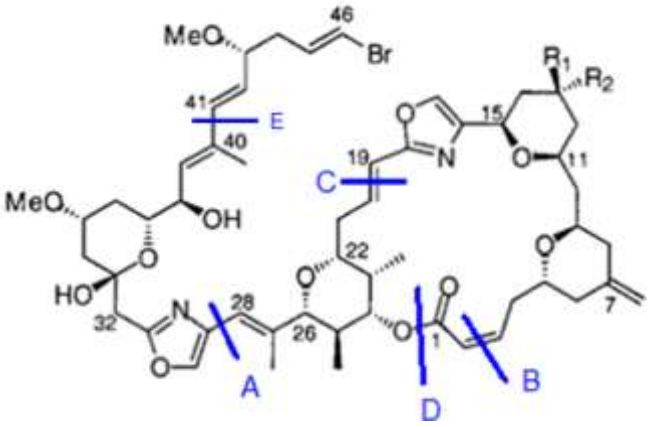

Figure 4. Analysis of bond breakage proposed by the Smith group. For A and E, they used Stille coupling. For B, they used Horner-Wadsworth-Emmons olefination. For C, they used Wittig olefination. D is just a ring closure reaction after attachment of an aldehyde (Dess-Martin oxidation) to the chain.

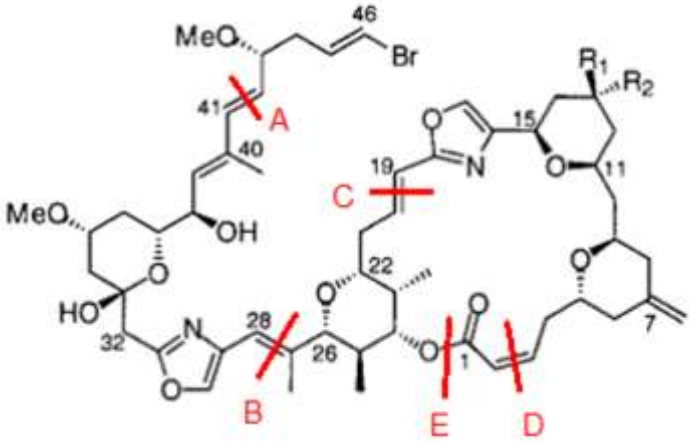

Figure 5. Analysis of bond breakage proposed by the Williams group. For A, they used Julia olefination. For B and D, they used Horner-Wadsworth-Emmons olefination. For C, they used Wittig olefination. E is just a ring closure reaction after the attachment of an aldehyde (Dess-Martin oxidation) to the chain.

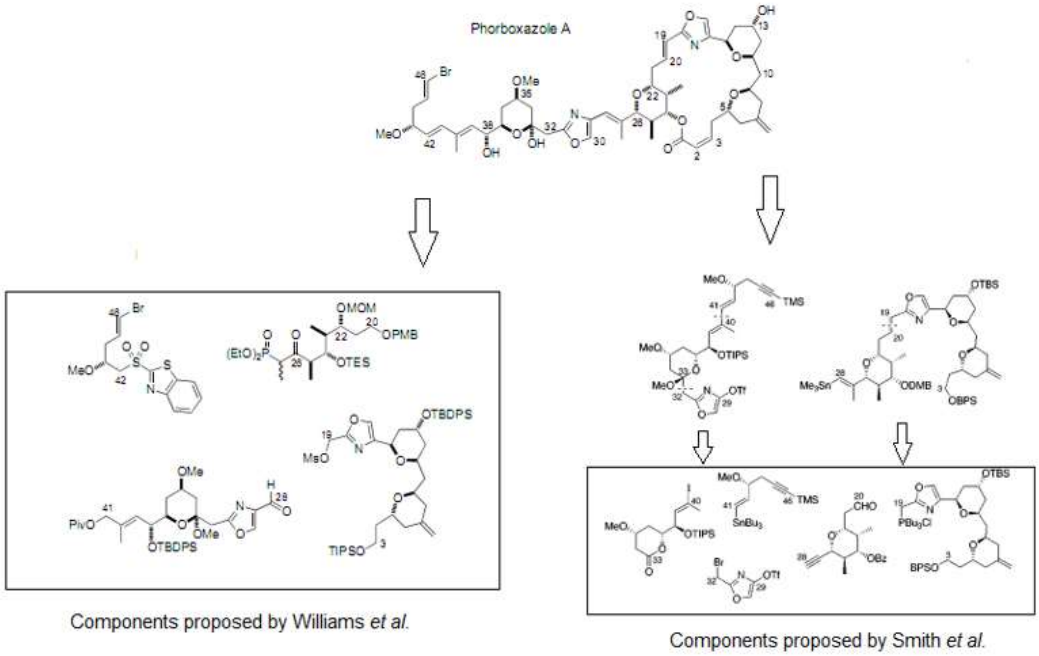

Figure 6. Components for the total synthesis of Phorboxazole A.

6. Stereocontrol, Oxazole Stability, and Macrocyclization

The total synthesis of phorboxazole A presents a stereochemical challenge, requiring the need for the precise control of 28 stereocenters. Strategies employed by different groups have relied heavily on iterative asymmetric allylation to construct tetrahydropyran subunits with defined 2,6-cis and 2,6-trans relationships, as shown in the syntheses of Williams and Smith. Convergent fragment assembly, often through stereoselective reactions (i.e., Petasis–Ferrier rearrangement), allowed each large fragment to be built with high stereochemical control. Intramolecular cyclizations, designed to take advantage of facial selectivity and pre-existing chiral centers, resulted in stereochemical configurations without racemization. The addition of the two oxazole rings has been shown through divergent strategies. The approach of the Smith group employed oxazole fragments that were incorporated during convergent coupling steps, necessitating the use of protecting-groups for the preservation of the integrity of oxazole during subsequent reactions [22]. Meanwhile, the Forsyth group leaned towards a biomimetic, *de novo* construction of oxazoles, which is often derived in situ from serine-derived amides via oxidation–cyclodehydration. This method improved stability and reduced the synthetic steps, avoiding the need of manipulating fully formed oxazole units until the late-stages of the synthesis [24]. The strategy is highly convergent, joining three preassembled fragments (e.g., C3–C17, C18–C30, C31–C46) in a modular fashion, allowing for analog generation by substituting individual fragments. Operationally, the bis-amidation/oxazole-forming sequence requires minimal manipulation of protecting-group, enabling the formation of both oxazoles in minimal steps from fragments. However, its modularity trade-offs include the complexity of preparing functionalized fragments, limited flexibility when altering scaffold regions outside the defined fragment boundaries, and the need for careful chemoselective control during the oxidation–cyclodehydration step.

Macrocyclization strategies also varies between the groups. The Williams group employed a late-stage lactonization strategy in which the macrocycle was closed in the final synthetic stages, typically via Julia olefination to install a Z-enoate. This maximized convergent fragment assembly prior to ring closure, though it required careful consideration of ring strain and functional group reactivities. On the other hand, the Smith group employed an early-stage macrocyclization strategy, forming the macrocyclic core prior to subsequent functionalization [22–23]. The comparative analysis, including the key strategic reactions, longest linear sequence, and overall yield of the major total synthesis strategies for Phorboxazole A is shown in Table 1.

The synthesis of phorboxazole B by Evans and Fitch follows a more traditional polyketide assembly approach, relying on asymmetric aldol reactions to construct key fragments, such as the C20–C38 and C39–C46 units in Part I, followed by the C1–C19 segment and final coupling in Part II [25]. The synthetic route, achieved in roughly 27 linear steps with an overall yield of about 12.6%, emphasizes stereochemical precision and stepwise control rather than biomimetic cyclization. Compared to phorboxazole A synthetic route by the Forsyth group, which forms oxazoles *de novo* in a highly convergent one-pot coupling, the Evans–Fitch approach is less step-economical but offers more direct control over stereochemical relationships and preinstalled heterocyclic features. In terms of route design, The Forsyth strategy was advantageous in terms of potential for analog synthesis, while the Evans and Fitch

strategy prioritizes stereocontrol and subunit, making the choice between them dependent on whether synthetic efficiency or precise stereochemical architecture was the primary goal.

Table 1. Comparative analysis of the major total synthesis strategies for Phorboxazole A.

Group	Key strategic reaction	Longest linear sequence (Steps)	Overall Yield	Reference
Smith	Petasis-Ferrier Rearrangement, Julia Olefination, Stille Coupling, Wittig Reaction	27	3.0	[22]
Williams	Convergent assembly, Horner-Wadsworth-Emmons Reaction, Wittig Reaction, Julia Olefination	10	80	[23]
Forsyth	*de novo* Oxazole Formation, Still-Gennari Olefination, Ring-Closing Metathesis	9	18	[24]
Evans (Phorboxazole B)	Asymmetric Aldol Reactions, Oxazole Reactivity Exploitation	27	12.6	[25]

7. Bioactivity

Phorboxazole A is one of the most potent naturally occurring anticancer macrolides, with promising cytostatic activity against various cancer cell lines. The structural complexity of phorboxazole A introduces challenges for organic chemists, including the construction of two oxazole heterocycles, multiple stereocenters, and the formation of tetrahydropyran rings with precise stereochemistry [41]. The challenges inspired the researchers to develop innovative and novel synthetic methodologies that led to broader applications in synthesizing related compounds. The Smith group at the University of Pennsylvania developed one of the first total syntheses of phorboxazole A through the use of a modified Petasis-Ferrier union/rearrangement tactic in constructing the complex tetrahydropyran rings embedded in the macrolide structure. Their approach utilized the stereocontrolled construction of the C11–C15 and C22–C26 cis-tetrahydropyran rings using the Petasis-Ferrier method, extension of the Julia olefination for the synthesis of enol ethers, application of a novel bifunctional oxazole linchpin, and Still coupling of a C28 trimethylstannane with a C29 oxazole triflate [22]. This approach achieved a 3% overall yield with the longest linear sequence of 27 steps. This was later improved to 4.6% overall yield with a reduced linear sequence of 24 steps. This second approach showed improved Petasis-Ferrier union/rearrangement conditions for multi-gram quantities of important tetrahydropyran intermediates [42]. Meanwhile, the Forsyth group developed a highly efficient approach featuring biomimetically inspired *de novo* oxazole formation, involving the convergent coupling of three fragments (C3–C17, C18–C30, and C31–C46) via biomimetic oxazole formation, assembly of the macrolide domain from C3–C17 and C18–C30 building blocks via the formation of the C16–C18 oxazole, macrolide ring closure using either an intramolecular Still-Gennari olefination or ring-closing metathesis, chemoselective one-pot bis-amidation sequence without amino or carboxyl protecting groups, and lastly, simultaneous formation of both oxazole moieties through oxidation-cyclodehydrations. This approach achieved an 18% overall yield in nine steps from the C3–C17 and C18–C30 fragments and is known as one of the most efficient synthetic routes to phorboxazole A. This approach

mimicked the proposed biosynthetic pathway, viewing the synthesis of phorboxazoles as mixed non-ribosomal peptide synthase/polyketide synthase products [43]. The Williams group, utilizing a highly convergent, stereocontrolled total synthesis of phorboxazole A, achieved an overall yield of 80% in just 10 steps. The asymmetric allylation reactions of stannyl-derived allyldiazaborolanes were demonstrated to be a key method for the enantiocontrolled assembly of functional components of phorboxazole A. Important features of this approach include a stereoselective cationic cyclization reaction for the formation of the fully substituted C22–C26 tetrahydropyran and the utilization of Julia olefination for the addition of the sensitive C37–C46 dienyl moiety [23].

Phorboxazole A exhibits exceptional cytostatic activity against cancer cell lines. Phorboxazole A is one of the most effective cytostatic drugs discovered, with a mean GI50 (growth inhibition) value of 1.58 nM against the National Cancer Institute (NCI) 's panel of 60 human cancer cell lines, selective suppression of HT29 (3.31×10^{-10} M) and HCT-116 (GI50 4.36×10^{-10} M) colon carcinoma cells, strong action against leukemia CCRF-CBM cell cultures (2.45×10^{-10} M), prostate cancer PC-3 (3.54×10^{-10} M), and breast cancer MCF7 (5.62×10^{-10} M). At the lowest test concentration of 1.6×10^{-9} M, the majority of the cell lines in the NCI panel were completely inhibited [17]. The mechanism of action of phorboxazole A differs from that of many other anticancer drugs. For example, it stops the cell cycle at the S phase in Burkitt lymphoma CA46 cultures, but it has no effect on microtubule stabilization or inhibition of microtubule polymerization, showing a new mechanism of action. Fluorescent derivatives of phorboxazole A have been used to separate binding proteins from HeLa cells, and phorboxazole analogs bind to cytokeratins, cyclin-dependent kinase 4 (cdk4), and a number of other proteins. Finally, the S phase cell cycle arrest may be caused by the sequestration of cdk4 on cytokeratin intermediate filaments. According to these results, phorboxazoles are a completely new class of cytostatic medicines that work differently from other well-known anticancer medications [17, 44].

Phorboxazole A is a promising lead chemical for the development of future anticancer drugs due to its remarkable potency and unique mechanism of action. The action of the chemical at sub-nanomolar concentrations raises the possibility of low-dose treatments with fewer adverse effects. Resistance to existing anticancer drugs may be overcome by its distinct mode of action. Additionally, phorboxazoles have antifungal and antibacterial properties, indicating possible uses outside of the treatment of cancer [45]. To fully understand the structure-activity relationship (SAR) of phorboxazole, several analogs have been produced due to significant synthetic efforts. With an IC50 of 2.25 ng/mL against HCT-116 cells, the congener (+)-44, which has an acetal substitution of the C-ring tetrahydropyran and C46 chloride, remained highly active. Potency was considerably decreased by the methyl ketal at C33 (IC50 of 92.6 ng/mL), highlighting the significance of the free hydroxyl at C33. A notable decrease in activity was demonstrated by hemi-phorboxazole A and a few additional analogs, revealing crucial structural components. SAR studies have directed the creation of simpler analogs with strong anticancer properties [9]. Another notable synthetic analog of phorboxazole A features C45–C46 vinyl chloride modifications, such as (+)-C(46)-chlorophorboxazole A, are potentially valuable in medicinal chemistry applications due to their antiproliferative properties against human cancer cell lines, often retaining or enhancing the cytostatic potency of the macrolide with picomolar inhibitory activity (e.g., GI50 values in the

pM range) comparable to phorboxazole A across the NCI's 60-tumor cell panel [19]. These approaches not only optimize analog synthesis but also support preliminary SAR findings that the C45–C46 vinyl chloride enhances cytotoxicity against diverse cancer types, paving the way for a more optimized medicinal applications. Table 2 shows the summary of the bioactivity of Phorboxazole A and its analogs.

Table 2. Summary of reported bioactivity of Phorboxazole A and its analogs.

Compound/Analog	Target Organism/Cell Line	Activity	Potency (IC_{50}/GI_{50})	Reference
Phorboxazole A	NCI-60 Human Cancer Cell Panel	Cytostatic	1.58 nM	[17]
Phorboxazole A	HCT-116 (Human Colon Tumor)	Cytostatic (GI_{50})	0.436 nM	[17]
Phorboxazole A	MCF7 (Human Breast Cancer)	Cytostatic (GI_{50})	0.562 nM	[17]
Phorboxazole A	*Candida albicans*	Antifungal	0.1 µg/disk	[5, 45]
Phorboxazole A	*Saccharomyces carlsbergensis*	Antifungal	0.1 µg/disk	[5, 45]
Hemi-phorboxazole A analogue (-)-4	HCT-116 (Colon) & SK-BR-3 (Breast)	Cytostatic	Nanomolar range	[16]
Hemi-phorboxazole A analogue (+)-3	*Candida albicans*	Antifungal	-	[16]
C-ring Acetal Analogue	HCT-116 (Colon)	Cytostatic (IC_{50})	2.25 ng/mL	[9]

8. Green Chemistry Strategies and Future Directions

For the phorboxazole A synthetic approaches of both the Smith group and Williams group, stereocontrol over multiple tetrahydropyran and other stereocenters was achieved through highly selective, stoichiometric, an assymetric allylations and cyclizations. Organocatalysis and metallocatalysis could serve as alternatives in streamlining these steps. Organocatalysts, such as chiral phosphoric acids, secondary amine/enamine catalysis, or oxa-Michael cascade reaction, can deliver high enantio- and diastereoselectivity without the need for metals, reducing purification burdens and environmental impact [46–48]. This is particularly true for fragment-level tetrahydropyran construction. Meanwhile, metal catalytic routes using chiral palladium, nickel, or other metals are useful for stereoselectivity [49]. A good strategy is to first evaluate organocatalysts for steps reliant on stoichiometric chiral reagents, and reserve metal catalysis for transformations where organocatalysis cannot match selectivity. The Stille coupling, used in earlier phorboxazole syntheses for fragment union, is highly efficient but also leads to serious environmental and safety drawbacks due to toxic organostannane reagents and challenging waste remediation. Greener alternatives, most notably the Suzuki–Miyaura coupling, could be potentially utilized due to comparable yields and stereochemical integrity while using boron reagents that are less toxic, more readily available, and easier to purify from reaction mixtures [50]. Hiyama couplings, which employ benign and bench-stable organosilanes, are another sustainable alternative, especially when used with green sovents and modern fluoride-free activation methods or copper co-catalysis that make them competitive with Stille in challenging cases [51]. Across all coupling options, greener processes, such as reduced catalyst loadings, alternative solvents, and continuous-flow operation, can significantly cut the environmental footprint while maintaining efficiency.

In terms of scalibility, the large-scale production of phorboxazole A or related analogs, replacing Stille couplings with Suzuki–Miyaura or modified Hiyama coupling reactions offers

the most industrially feasible path [52–53]. Both strategies are already employed in the pharmaceutical industry because they minimize toxic residues, simplify product purification, and use reagents compatible with greener process solvents and catalyst recycling. The convergent nature of the Smith and Williams approach is inherently favorable for scale-up, and with process optimization, including lower palladium loadings (down to the ppm range), ligand/solvent screening for rate acceleration, and early monitoring of residual metals, the synthetic route can be adapted to kilogram-scale synthesis. Continuous-flow processing provides additional advantages in heat/mass transfer, and catalyst load reduction [54]. By integrating these adjustments, the synthesis can meet both regulatory and cost constraints while maintaining the complex stereochemical structure inherent to phorboxazole A.

9. Conclusions

The total syntheses of phorboxazole A by the Smith and Williams groups features the Petasis-Ferrier union/rearrangement, crucial for stereocontrolled tetrahydropyran assembly. The Smith group used Stille coupling and Wittig olefination. Meanwhile, the Williams group followed a convergent Horner-Wadsworth-Emmons and Julia olefination approaches. Lastly, the Forsyth group employed biomimetic *de novo* oxazole formation highlighting modularity for analogs. The biological activity of Phorboxazole A, particularly its nanomolar cytostatic effects against NCI-60 cancer lines and antifungal potency against *Candida albicans*, emphasizes its advantage as a novel antimitotic, with analogs like C45–C46 vinyl chloride derivatives retaining picomolar activity. Incorporating green chemistry strategies, through organocatalysis for asymmetric allylations, Suzuki-Miyaura couplings to replace toxic Stille reactions, and continuous-flow processes, could help mitigate environmental impacts, enhance scalability, and pave the way for sustainable production of phorboxazole analogs and derivatives, leading to a more optimized drug development processes against resistant cancers and infections while aligning with eco-friendly pharmaceutical innovation.

Acknowledgments

No funding received for this work

Author Contribution

Jovale Vincent Tongco: conceptualization, literature search, writing, review, and editing

Competing Interest

The author declares that there are no competing interests, financial or otherwise, that could influenceor bias the content of this review article.

Appendix A. Supplementary Materials

Supplementary Materials to this article can be found online at https://doi.org/10.53623/sein.v2i2.789.

References

[1] Vannuffel, P.; Cocito, C. (1996). Mechanism of action of streptogramins and macrolides. *Drugs, 51*, 20–30. https://doi.org/10.2165/00003495-199600511-00006.

[2] Van Bambeke, F.; Tulkens, P.M. (2001). Macrolides: pharmacokinetics and pharmacodynamics. *International Journal of Antimicrobial Agents, 18,* 17–23. https://doi.org/10.1016/S0924-8579(01)00406-X.

[3] Retsema, J.; Fu, W. (2001). Macrolides: structures and microbial targets. *International Journal of Antimicrobial Agents, 18,* 3–10. https://doi.org/10.1016/S0924-8579(01)00401-0.

[4] Mazzei, T.; Mini, E.; Novelli, A.; Periti, P. (1993). Chemistry and mode of action of macrolides. *Journal of Antimicrobial Chemotherapy, 31*, 1–9. https://doi.org/10.1093/JAC/31.SUPPL_C.1.

[5] Searle, P.A.; Molinski, T.F. (1995). Phorboxazoles A and B: Potent Cytostatic Macrolides from Marine Sponge *Phorbas* Sp. *Journal of the American Chemical Society, 117*, 8126–8131. https://doi.org/10.1021/JA00136A009.

[6] Kulkarni, S.; Kaur, K.; Jaitak, V. (2021). Recent Developments in Oxazole Derivatives as Anticancer Agents: Review on Synthetic Strategies, Mechanism of Action and SAR Studies. *Anti-Cancer Agents in Medicinal Chemistry, 22*, 1859–1882. https://doi.org/10.2174/1871520621666210915095421.

[7] Li, S.; Mei, Y.; Jiang, L.; *et al.* (2025). Oxazole and isoxazole-containing pharmaceuticals: targets, pharmacological activities, and their SAR studies. *RSC Medicinal Chemistry*, *16*, 1879-1890. https://doi.org/10.1039/D4MD00777H.

[8] Zhang, H.Z.; Zhao, Z.L.; Zhou, C.H. (2018). Recent advance in oxazole-based medicinal chemistry. *European Journal of Medicinal Chemistry, 144,* 444–492. https://doi.org/10.1016/J.EJMECH.2017.12.044.

[9] Smith, A.B.; Hogan, A.M.L.; Liu, Z.; *et al*. (2011). Phorboxazole synthetic studies: design, synthesis and biological evaluation of phorboxazole A and hemi-phorboxazole A related analogues. *Tetrahedron, 67,* 5069–5078. https://doi.org/10.1016/J.TET.2010.12.043.

[10] Searle, P.A.; Molinski, T.F.; Brzezinski, L.J.; Leahy, J.W. (1996). Absolute configuration of phorboxazoles A and B from the marine sponge Phorbas sp. 1. Macrolide and hemiketal rings. *Journal of the American Chemical Society, 118*, 9422–9423. https://doi.org/10.1021/JA962092R.

[11] Limas, J.C.; Cook, J.G. (2019). Preparation for DNA Replication: The Key to a Successful S phase. *FEBS Letters, 593,* 2853. https://doi.org/10.1002/1873-3468.13619.

[12] Nasheuer, H.P.; Meaney, A.M. (2024). Starting DNA Synthesis: Initiation Processes during the Replication of Chromosomal DNA in Humans. *Genes*, 15, 360. https://doi.org/10.3390/GENES15030360.

[13] Matthews, H.K.; Bertoli, C.; de Bruin, R.A.M. (2021). Cell cycle control in cancer. *Nature Reviews Molecular Cell Biology, 23,* 74–88. https://doi.org/10.1038/s41580-021-00404-3.

[14] Li, S.; Wang, L; Wang, Y.; *et al*. (2022). The synthetic lethality of targeting cell cycle checkpoints and PARPs in cancer treatment. *Journal of Hematology & Oncology, 15,* 1–32. https://doi.org/10.1186/S13045-022-01360-X.

[15] Bhowmick, R.; Hickson, I.D.; Liu, Y. (2023). Completing genome replication outside of S phase. *Molecular Cell, 83,* 3596–3607. https://doi.org/10.1016/J.MOLCEL.2023.08.023.

[16] Smith, A.B.; Liu, Z.; Hogan, A.M.L., *et al*. (2009). Hemi-phorboxazole A: Structure confirmation, analogue design and biological evaluation. *Organic Letters, 11,* 3766–3769. https://doi.org/10.1021/OL9014317.

[17] Williams, D.R.; Kiryanov, A.A.; Emde, U.; *et al*. (2004). Studies of stereocontrolled allylation reactions for the total synthesis of phorboxazole A. *Proceedings of the National Academy of*

Sciences of the United States of America, 101, 12058–12063. https://doi.org/10.1073/PNAS.0402477101.

[18] Shultz, Z.; Leahy, J.W. (2016). Synthesis of the phorboxazoles—potent, architecturally novel marine natural products. *The Journal of Antibiotics, 69,* 220–252. https://doi.org/10.1038/ja.2016.8.

[19] Smith, A.B.; Razler, T.M.; Meis, R.M.; Pettit, G.R. (2008). Synthesis and biological evaluation of phorboxazole congeners leading to the discovery and preparative-scale synthesis of (+)-chlorophorboxazole A possessing picomolar human solid tumor cell growth inhibitory activity. *Journal of Organic Chemistry, 73* 1201–1208. https://doi.org/10.1021/JO701816H.

[20] do Amaral, B.S.; da Silva. F.B.; Leme, G.M.; *et al*. (2021). Integrated analytical workflow for chromatographic profiling and metabolite annotation of a cytotoxic Phorbas amaranthus extract. *Journal of Chromatography B, 1174,* 122720. https://doi.org/10.1016/J.JCHROMB.2021.122720.

[21] Caso, A.; da Silva, F.B.; Esposito, G.; *et al*. (2021). Exploring Chemical Diversity of Phorbas Sponges as a Source of Novel Lead Compounds in Drug Discovery. *Marine Drugs, 19,* 667. https://doi.org/10.3390/MD19120667.

[22] Smith, A.B.; Minbiole, K.P.; Verhoest, P.R.; Schelhaas, M. (2001). Total synthesis of (+)-phorboxazole A exploiting the Petasis-Ferrier rearrangement. *Journal of the American Chemical Society, 123,* 10942–10953. https://doi.org/10.1021/JA011604L.

[23] Williams, D.R.; Kiryanov, A.A.; Emde, U.; *et al*. (2003). Total Synthesis of Phorboxazole A. *Angewandte Chemie International Edition, 42,* 1258–1262. https://doi.org/10.1002/ANIE.200390322.

[24] Forsyth, C.J.; Ahmed, F.; Cink, R.D.; Lee, C.S. (1998). Total synthesis of phorboxazole A. J Am Chem Soc 120:5597–5598. https://doi.org/10.1021/JA980621G.

[25] Evans, D.A.; Fitch, D.M.; Smith, T.E.; Cee, V.J. (2000) Application of complex aldol reactions to the total synthesis of phorboxazole B. *Journal of the American Chemical Society, 122,* 10033–10046. https://doi.org/10.1021/JA002356G.

[26] Desriac, F.; Jégou, C.; Balnois, E.; *et al*. (2013). Antimicrobial Peptides from Marine Proteobacteria. *Marine Drugs, 11*,3632–3660. https://doi.org/10.3390/MD11103632.

[27] Mizuno, C.M.; Kimes, N.E.; López-Pérez, M.; *et al.* (2013). A Hybrid NRPS-PKS Gene Cluster Related to the Bleomycin Family of Antitumor Antibiotics in Alteromonas macleodii Strains. *PLoS One, 8*, e76021. https://doi.org/10.1371/JOURNAL.PONE.0076021.

[28] Zhu, P.; Zheng, Y.; You, Y.; *et al*. (2009). Sequencing and modular analysis of the hybrid non-ribosomal peptide synthase – polyketide synthase gene cluster from the marine sponge Hymeniacidon perleve-associated bacterium Pseudoalteromonas sp. strain NJ631. *Canadian Journal of Microbiology, 55,* 219–227. https://doi.org/10.1139/W08-125.

[29] Motoyoshiya, J.; Kusaura, T.; Kokin, K.; *et al*. (2001). The Horner–Wadsworth–Emmons reaction of mixed phosphonoacetates and aromatic aldehydes: geometrical selectivity and computational investigation. *Tetrahedron, 57*, 1715–1721. https://doi.org/10.1016/S0040-4020(01)00007-2.

[30] Trippett, S. (1963). The Wittig reaction. *Quarterly Reviews, Chemical Society, 17,* 406–440. https://doi.org/10.1039/QR9631700406.

[31] Lao, Z.; Toy, P.H. (2016). Catalytic Wittig and aza-Wittig reactions. *Beilstein Journal of Organic Chemistry, 12,* 253 12:2577–2587. https://doi.org/10.3762/BJOC.12.253.

[32] Byrne, P.A.; Gilheany, D.G. (2013). The modern interpretation of the Wittig reaction mechanism. *Chemical Society Reviews, 42,* 6670–6696. https://doi.org/10.1039/C3CS60105F.

[33] Maercker, A. (2011). The Wittig Reaction. *Organic Reactions*, 270–490. https://doi.org/10.1002/0471264180.OR014.03.

[34] Minbiole, E.C.; Minbiole, K.P.C. (2016). The Petasis-Ferrier rearrangement: developments and applications. *The Journal of Antibiotics, 69,* 213–219. https://doi.org/10.1038/ja.2015.136.

[35] Ferrier, R.J. (1979). Unsaturated carbohydrates. Part 21. A carbocyclic ring closure of a hex-5-enopyranoside derivative. *Journal of the Chemical Society, Perkin Transactions 1,* 1455–1458. https://doi.org/10.1039/P19790001455.

[36] Ilia, G.; Simulescu, V.; Plesu, N; Chiriac, V.; Merghes, P. (2023). Wittig and Wittig–Horner Reactions under Sonication Conditions. *Molecules, 28,* 1958. https://doi.org/10.3390/MOLECULES28041958.

[37] Plesniak, K.; Zarecki, A.; Wicha, J. (2006). The Smiles Rearrangement and the Julia–Kocienski Olefination Reaction. *Topics in Current Chemistry, 275,* 163–250. https://doi.org/10.1007/128_049.

[38] Mirk, D.; Grassot, J.M.; Zhu, J. (2006). Synthesis of 4-nitrophenyl sulfones and application in the modified Julia olefination. *Synlett, 2006,* 1255–1259. https://doi.org/10.1055/S-2006-939682.

[39] Chrenko, D.; Pospíšil, J. (2024). Latest Developments of the Julia–Kocienski Olefination Reaction: Mechanistic Considerations. *Molecules, 29,* 2719. https://doi.org/10.3390/molecules29122719.

[40] Blakemore, P.R. (2002). The modified Julia olefination: alkene synthesis via the condensation of metallated heteroarylalkylsulfones with carbonyl compounds. *Journal of the Chemical Society, Perkin Transactions 1, 2,* 2563–2585. https://doi.org/10.1039/B208078H.

[41] Wang, B.; Hansen, T.M.; Wang, T.; *et al*. (2011). Total synthesis of phorboxazole A via *de novo* oxazole formation: Strategy and component assembly. J Am Chem Soc 133:1484–1505. https://doi.org/10.1021/JA108906E.

[42] Smith, A.B.; Razler, T.M.; Ciavarri, J.P.; *et al*. (2008). A second-generation total synthesis of (+)-phorboxazole A. *Journal of Organic Chemistry, 73,* 1192–1200. https://doi.org/10.1021/JO7018152.

[43] Wang, B.; Hansen, T.M.; Weyer, L.; *et al*. (2011). Total synthesis of phorboxazole a via *de novo* oxazole formation: Convergent total synthesis. *Journal of the American Chemical Society, 133,* 1506–1516. https://doi.org/10.1021/JA1089099.

[44] Forsyth, C.J.; Ying, L.; Chen, J.; La Clair, J.J. (2006). Phorboxazole analogues induce association of cdk4 with extranuclear cytokeratin intermediate filaments. *Journal of the American Chemical Society, 128,* 3858–3859. https://doi.org/10.1021/JA057087E.

[45] Donia, M.; Hamann, M.T. (2003). Marine natural products and their potential applications as anti-infective agents. *Lancet Infectious Diseases, 3*, 338–348. https://doi.org/10.1016/S1473-3099(03)00655-8.

[46] Terada, M. (2010). Chiral Phosphoric Acids as Versatile Catalysts for Enantioselective Transformations. *Synthesis, 12*, 1929–1982. https://doi.org/10.1055/s-0029-1218801.

[47] Nair, V.V.; Arunprasath, D.; Pandidurai, S.; Sekar, G. (2022). Synergistic Dual Amine/Transition Metal Catalysis: Recent Advances. *European Journal of Organic Chemistry, 23*, e202200244. https://doi.org/10.1002/ejoc.202200244.

[48] Wang, Y.; Du, D. (2020). Recent advances in organocatalytic asymmetric oxa-Michael addition triggered cascade reactions. *Organic Chemistry Frontiers, 7*, 3266–3283. https://doi.org/10.1039/D0QO00631A.

[49] Yorimitsu, H.; Kotora, M.; Patil, N.T. (2021). Special Issue: Recent Advances in Transition-Metal Catalysis. *The Chemical Record, 21*, 3335–3337. https://doi.org/10.1002/tcr.202100305.

[50] Hie, L.; Chang, J.J.; Garg, N.K. (2014). Nickel-Catalyzed Suzuki–Miyaura Cross-Coupling in a Green Alcohol Solvent for an Undergraduate Organic Chemistry Laboratory. *Journal of Chemical Education, 92*, 571–574. https://doi.org/10.1021/ed500158p.

[51] Noor, R.; Zahoor, A.F.; Irfan, M,; *et al*. (2022). Transition Metal Catalyzed Hiyama Cross-Coupling: Recent Methodology Developments and Synthetic Applications. *Molecules, 27*, 5654. https://doi.org/10.3390/molecules27175654.

[52] Blakemore, D. (2016). Suzuki–Miyaura Coupling. In Synthetic Methods in Drug Discovery, Vol. 1.; Blakemore, D.C.; Doyle, P.M.; Fobian, Y.M.; *et al*. Royal Society of Chemistry: London, UK,; 1–69. https://doi.org/10.1039/9781782622086.

[53] Li, M.; Tsui, G.V. (2023). Stereoselective Palladium-Catalyzed Hiyama Cross-Coupling Reaction of Tetrasubstituted *gem*-Difluoroalkenes. *Organic Letters, 26*, 376–379. https://doi.org/10.1021/acs.orglett.3c04037.

[54] Rahman, R.; Malik, F.; Hein, Z.M.; *et al*. (2024). Continuous Flow Synthesis and Applications of Metal-Organic Frameworks: Advances and Innovation. *ChemPlusChem, 90*, e202400634. https://doi.org/10.1002/cplu.202400634.